Improvement of seismicity parameters in the Arabian Shield and Platform using earthquake location and magnitude calibration

A. M. Al-Amri and A. J. Rodgers

Keywords

Earthquake location • Magnitude • Saudi Arabia • Arabian shield • Gulf of Aqabah • Platform • Focal mechanism

---

Introduction

There has only been a modest amount of earthquake seismological work done in the Arabian Peninsula. Several countries either on or surrounding the Peninsula have seismograph stations, but most stations are equipped with short-period vertical seismometers. In any event, the networks are sparse and often are poorly situated with respect to seismically active areas. Broadband data required for analysis of teleseismic receiver functions are almost wholly lacking. Regional wave propagation from earthquakes and seismic wave attenuation have not been studied. Microseismicity is known to occur in many areas of the Peninsula, but the existing network of stations is inadequate for accurately defining spatial characteristics or determining focal mechanisms.

One of the main objectives of this study was to estimate crustal and upper mantle structure to improve earthquake location and magnitude estimation. While there have been many studies on this topic using a wide variety of techniques, many questions about the structure on the Arabian Peninsula remain unanswered. A thorough understanding of the seismic structure and wave propagation characteristics of the region must be established before proceeding to assess the seismic hazard. Therefore, the objective of the proposed research was to improve assessment of seismic hazard parameters by improving earthquake location and magnitude estimates with the KACST seismic network.

Seismotectonics and Seismic Structure

The Arabian Peninsula forms a single tectonic plate, the Arabian Plate. It is surrounded on all sides by active plate boundaries as evidenced by earthquake locations. Figure 14.1 shows a map of the Arabian Peninsula along with major tectonic features and earthquake locations. Active tectonics of the region is dominated by the collision of the Arabian Plate with the Eurasian Plate along the Zagros and Bitlis Thrust systems, rifting and seafloor spreading in the Red Sea and Gulf of Aden. Strike-slip faulting occurs along the Gulf of Aqabah and Dead Sea Transform fault systems. The great number of earthquakes in the Gulf of Aqabah poses a significant seismic hazard to Saudi Arabia. Large earthquakes in the Zagros Mountains of southern Iran may lead to long-period ground motion in eastern Saudi Arabia.

The two large regions associated with the presence or absence of a sedimentary cover define the large scale geologic structure of the Arabian Peninsula. The Arabian Platform (eastern Arabia) is covered by sediments that thicken toward the Arabian Gulf. The Arabian Shield has no appreciable sedimentary cover with many outcrops. The northwestern regions of Saudi Arabia are distinct from the Arabian Shield, as this region is characterized by high seismicity in the Gulf of Aqabah and Dead Sea Rift. Active tectonics in this region is associated with the opening of the northern Red Sea and Gulf of Aqabah as well as a major continental strike-slip plate boundary.

The Dead Sea transform system connects active spreading centers of the Red Sea to the area where the Arabian Plate is converging with Eurasia in southern Turkey. The Gulf of Aqabah in the southern portion of the rift system has experienced left-lateral strike-slip faulting with a 110 km offset since early Tertiary to the present. The seismicity of the Dead Sea transform is characterized by both swarm and mainshock-aftershock types of earthquake activities.

A. M. Al-Amri (✉)
Deptartment of Geology, King Saud University, Riyadh 11451, Saudi Arabia
e-mail: amsamri@ksu.edu.sa

A. J. Rodgers
Atmosphere, Earth and Energy Department, Lawrence Livermore National Laboratory, University of California, Livermore, CA 94551, USA

Fig. 14.1 Map of the Arabian peninsula and surrounding regions. Major geographic and tectonic/geologic features are indicated. Plate boundaries are indicated by *yellow lines*. Earthquakes and volcanic centers are shown as *red circles* and *yellow diamond*, respectively

● Earthquake - reported by USGS-NEIC-PDE
◇ Volcanic Center
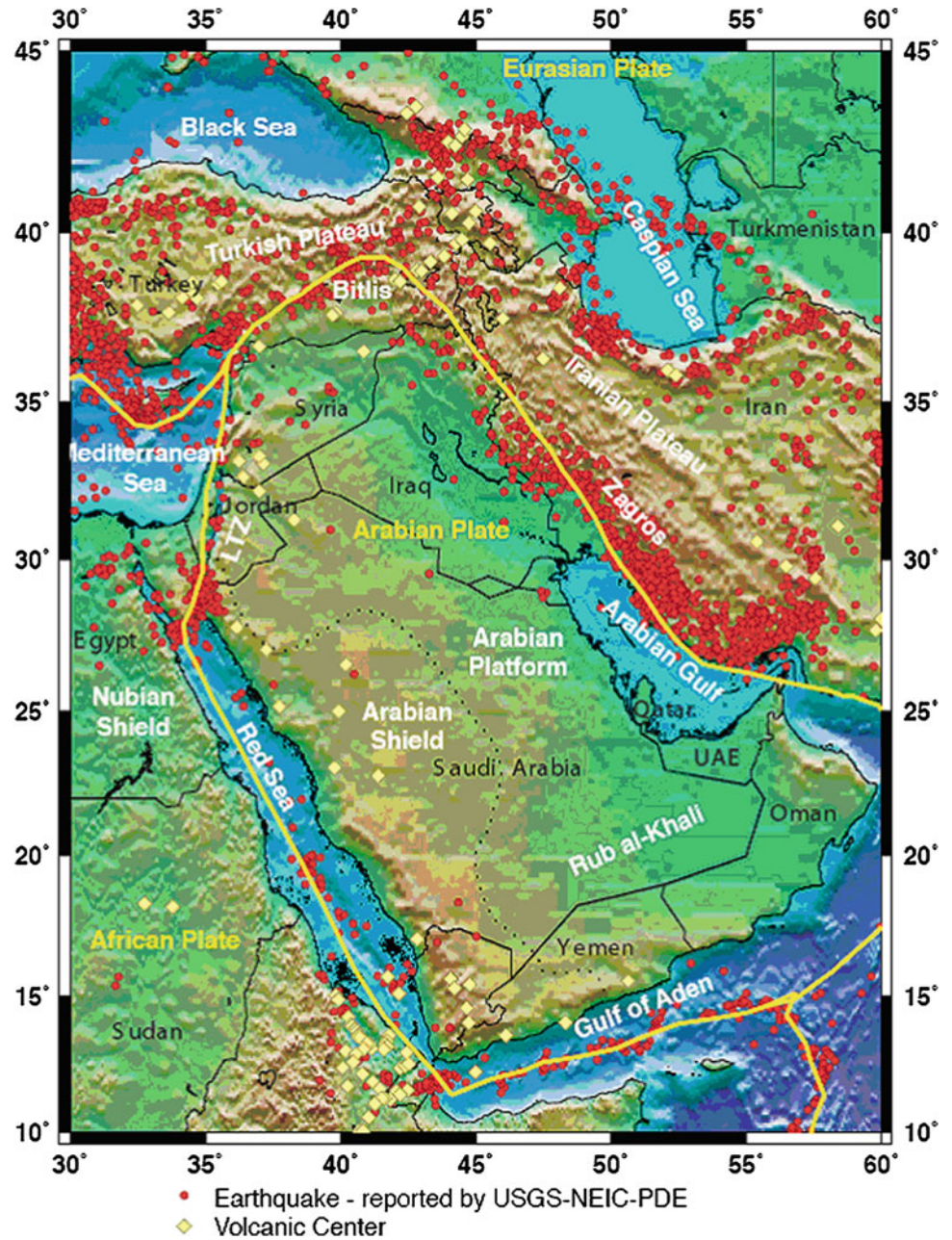
The Arabian Plate boundary extends east-northeast from the Afar region through the Gulf of Aden and into the Arabian Sea and Zagros fold belt. The boundary is clearly delineated by teleseismic epicenters, although there are fewer epicenters bounding the eastern third of the Arabian Plate south of Oman. Most seismicity occurs in the crustal part of the Arabian Plate beneath the Zagros folded belt (Jackson and Fitch 1981). The Zagros is a prolific source of large magnitude earthquakes with numerous magnitude 7+ events occurring in the last few decades. The overall lack of seismicity in the interior of the Arabian Peninsula suggests that little internal deformation of the Arabian Plate is presently occurring. Mooney et al. (1985) suggest that the

geology and velocity structure of the Shield can be explained by a model in which the Shield developed in the Precambrian by suturing of island arcs. They interpreted the boundary between the eastern shield and the Arabian Platform as a suture zone between crustal blocks of differing composition. Surface waves observed at the long-period analog stations RYD (Riyadh), SHI (Shiraz, Iran), TAB (Tabriz, Iran), HLW (Helwan, Egypt), AAE (Addis-Ababa, Ethiopia) and JER (Jerusalem) were used to estimate crustal and upper mantle structure (Seber and Mitchell 1992), (Mokhtar and Al-Saeed 1994) These studies reported faster crustal velocities for the Arabian Shield and slower velocities for the Arabian Platform.

The Saudi Arabian Broadband Deployment (Vernon and Berger 1997; Al-Amri et al. 1999) provided the first data set of broadband recordings of this region. This deployment consisted of nine broadband three-component seismic stations along a similar transect an early seismic refraction study (Mooney et al. 1985; Gettings et al.1986). Data from the experiment resulted in several studies and models (Sandvol et al. 1998; Mellors et al. 1999; Rodgers et al. 1999; Benoit et al. 2002). These studies provided new constraints on crustal and upper mantle structure. The crustal model of the western Arabian Platform shows a little higher P-velocity for the upper crust in the Shield than in the Platform and the crustal Platform seems to have a greater thickness than in the Shield by about 3 km. The Moho discontinuity beneath the western Arabian Platform indicates a velocity of 8.2 km/sec of the upper mantle and 42 km depth (Al-Amri 1998; Al-Amri 1999).

Generally, the crustal thickness in the Arabian Shield area varies from 35 to 40 km in the west adjacent to the Red Sea to 45 km in central Arabia (Sandvol et al.1998; Rodgers et al. 1999). Not surprising the crust thins nears the Red Sea (Vernon and Berger 1997; Gettings et al. 1986; Mellors et al.1999). High-frequency regional S-wave phases are quite different for paths sampling the Arabian Shield than those sampling the Arabian Platform (Mellors et al. 1999; Sandvol et al. 1998). In particular the mantle Sn phase is nearly absent for paths crossing parts of the Arabian Shield, while the crustal Lg phase is extremely large amplitude. This may result from an elastic propagation effect or extremely high mantle attenuation and low crustal attenuation occurring simultaneously, or a combination of both.

Previous reports of large scale seismic structure (Ritsema et al.1999; Debayle et al. 2001) suggest that a low velocity anomaly in the upper mantle extends laterally beneath the Arabian Shield from the Red Sea in the west to the shield—platform boundary in the east. Additionally, Debayle et al. (2001) observe a narrow region of low velocity beneath the Red Sea and western edge of the Arabian Shield, extending to 650 km depth. A recent tomographic velocity model and receiver function analysis by (Benoit et al. 2002) suggests the upper mantle low velocity anomaly is smaller in extent, laterally and vertically, than imaged in previous studies.

Seismic Techniques

The study improved the earthquake location and magnitude estimates using waveform data from KACST digital seismic network. The proposed research includes standard seismological investigations as well as newly developed techniques as follows:

Data Collection and Validation

In order to validate the station timing and instrument response we performed comparisons of timing and amplitudes of P-waves for large teleseismic events at KACST stations with the Global Seismic Station RAYN. This station has well calibrated timing and instrument response. The relative arrival times of teleseismic P-waves at KACST stations can be accurately measured by cross-correlating with the observed waveforms at RAYN and correcting for distance effects. Absolute amplitudes of teleseismic P-waves at the KACST and RAYN stations were measured by removing the instrument response and gain and band-pass filtering.

This study also considered many events and computed average travel time and amplitude residuals relative to a globally averaged 1D earth model, such as iasp9l. Although there were deviations between the timing and amplitudes of KACST P-waves from the predictions of the iasp9I model (because of lateral heterogeneity) the tests were useful to identify which stations might have timing and/or instrument calibration problems.

Travel Time Calibration

One of the most fundamental elements of seismological research is earthquake location. In fact the main product of any seismic network is the reporting of earthquake location, origin time and magnitude. The first major element of our proposed research was to improve earthquake locations by developing and improving models of the seismic velocity structure. It is well known that the lithosphere (crust and uppermost mantle) of Saudi Arabia is heterogeneous. Some of the difference in the seismically inferred crustal structure of eastern and western Arabia is due to the thick sediments of the Arabian Platform. However, waveform modeling results (Rodgers et al. 1999) suggest that there are also differences in the seismic velocities of the crystalline crust between the Arabian Shield and Platform. These differences result in travel time variations within the Arabian Peninsula, which will bias earthquake locations when a single, one—dimensional velocity model is used.

Similarly, there are variations in the amplitudes of regional phases, such as those reported by Mellors et al. (1999). That study reported that Pn, Pg and Sn body-waves from the Gulf of Aqabah events to central Arabia are weak, while the Lg phase along this path is strong. More normal continental energy partitioning of the regional phases is observed for earthquakes from the Zagros. These variations in regional phase propagation characteristics can make it difficult to develop detection algorithms for regional phases,

most importantly the first arriving Pn phase. The fundamental travel time and amplitude behavior of regional phases needs to be characterized before the KACST stations can be tuned to provide optimal phase detection, locations and magnitudes.

Accordingly, we improved the earthquake location and origin time estimates by developing and improving models of the regional seismic phases and the seismic velocity structure of the lithosphere. Firstly, we collected data from large well-observed earthquakes with well-constrained locations, depths and origin times. We selected events with more than 50 stations and have an open-azimuth of less than 90° which are located within 20 km of ground truth locations. We reviewed travel time picks of regional phases Pn, Pg, Sn and Lg and quality controlled before they are included into the data set. Travel time curves for each phase were generated. As sufficient data are collected, we developed regional travel time models for different paths (e.g. Arabian Shield and Arabian Platform) and for events in different source regions (e.g. Gulf of Aqabah, Red Sea, Zagros Mountains).

Focal Mechanism Solutions and Refinement of Velocity Models

In order to develop a robust magnitude scale, earthquake moments, focal mechanisms and depths were estimated by modeling observed long-period three-component waveforms (Walter 1993). We modeled the observed waveforms with complete reflectivity synthetic seismograms (Randall 1994) using an appropriate seismic velocity model of the crust and shallow mantle. The current models were validated (Rodgers et al. 1999), in order to possibly refine them or develop new models. Special efforts were spent to define the regions of validity of the velocity models.

Firstly, we considered large earthquakes (Mw > 5.0) that are within regional distance (<1,500 km) of Saudi Arabia. Often events of this size have focal parameters from global observations (such the Harvard GMT or USGS-NEIC moment tensor projects). Waveform data for these events were selected and reviewed for signal-to-noise. The data were corrected for instrument response, converted to ground displacement and the horizontals were rotated to radial and transverse components.

Earthquake focal mechanism, depth and seismic moment were estimated by fitting synthetic seismograms to the long-period three-component waveforms. The source parameters are estimated by a grid search method (Walter 1993). For a series of depths, all possible orientations of the double couple focal mechanism (strike, dip and rake) are investigated.

Seismographic Networks

King Abdulaziz City for Science and Technology (KACST) operates a network of three-component broadband and short-period stations (Al-Amri and Al-Amri 1999). The network has stations throughout the Kingdom of Saudi Arabia, but the station density is greatest near the Gulf of Aqabah. The network recorded the shots with good signal-to-noise above about 0.5 Hz. And runs the Boulder Real Time Technologies (BRTT) Antelope System as described below.

ANTELOPE is a system of software modules that implement acquisition, transport, buffering, processing, archiving and distribution of environmental monitoring information. Antelope is a distributed, open-architecture, UNIX-based acquisition, analysis and management system. It consists of two major sub-systems, namely Antelope Real Time System **(ARTS)** and Antelope Seismic Information System **(ASIS)**. ARTS brings raw data from remote field sites in real time to KSU processing center where, automated real time processing of data is performed and information is automatically merged into long-term information system archives. Within ARTS, data is buffered and transported through a mechanism known as an Object Ring Buffer (ORB), which acts as the heart of ARTS. The ORB is managed by a single program, "obrserver". Field interface modules write all of the data from the field stations into the ORB. The concepts behind an ORB are straightforward:

(1) A circular raw data store on disk.
(2) A server-client approach to manage the circular data store.
(3) All server-client inter-process communications take place through Internet sockets using TCP/IP.

Real time Richter magnitude estimates are made by a module called "orbmag". This program looks for ASIS origin rows data in the data processing ORB. For each origin read, orbmag determines appropriate time windows for each station and acquires the waveform data for all components from the same data processing ORB. Each waveform segment is converted to equivalent drum recorder displacement of a standard Wood-Anderson instrument and the maximum amplitude for the event is determined. These amplitudes are fed into the standard Richter magnitude formula for computing ml values for each station and all of the station ml values are median averaged to get a total network ml estimate. The ml estimate is used to modify the input origin row and this modified origin row is written back into the data processing ORB. Location capability is provided by program "orbgenloc" which uses traditional inversion algorithm. The program "orbenloc" provides a generic location capability using traditional inversion algorithms. In addition, locations produced by "orbassoc"
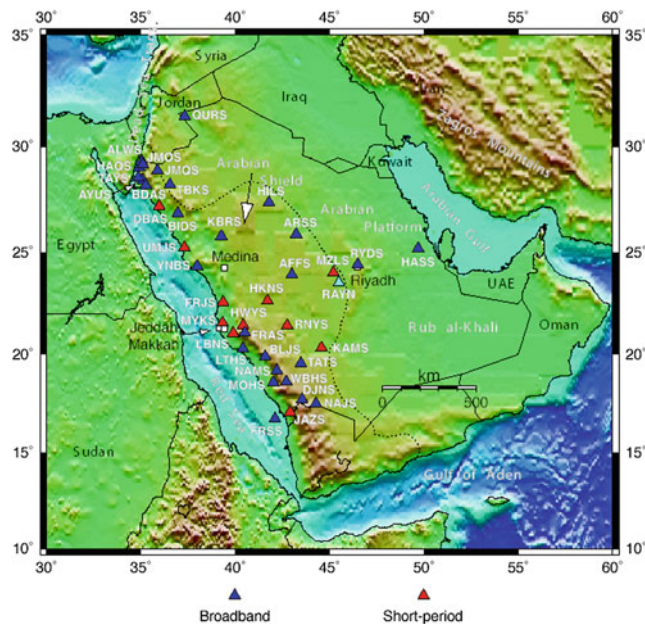
Fig. 14.2 Location map of KACST digital seismic network

module can be fine tuned with "*orbgenloc*". "*orbgenloc*" reads the arrival, association and preliminary hypocenter information produced by "*orbassoc*" and computes a more refined earthquake location using a variety of traditional inversion algorithms. The refined locations are written to an output ORB as database row packets.

KACST Seismographic Network

In May 1998 King Abdulaziz City for Science and Technology (KACST) began operating the digital seismic network. A description of the network is given in Al-Amri and Al-Amri (1999). It consists of 38 stations mostly distributed across the Arabian Shield (western Saudi Arabia, Fig. 14.2). The instrumentation features 27 broadband and 11 short-period instruments. The station information is compiled in Table 14.1. All stations record three-component ground motions at a sample rate of 100 samples/second. The stations operate continuously and transmit data in real-time to the KACST Headquarters building in Riyadh. The KACST Data Center receives the raw waveform data and runs the Boulder Real Time Technologies (BRTT) Antelope System. This is a software package for managing real-time seismic network data and performing the basic network operations of detection, association and location of events as well as data archival. A short-term average-to-long-term average (STA/LTA) energy detector runs continuously and detects phase arrivals. The system attempts to locate the event if a number of arrivals are detected by the network within a specified time window. The system locates events relative

to a single average global velocity model (*iasp91*, Kennett and Engdahl 1991).

GSN Seismic Station

RAYN is one of the newest stations in the IRIS/IDA global seismographic network. The seismic station at Ar Rayn (RAYN), Saudi Arabia was established in 1996 under a memorandum of understanding between KACST, the IRIS Consortium, and the University of California, San Diego (UCSD), with key support from the KSU Department of Geology.

RAYN station consists of a STS-2 three-component broadband seismometer (passband between 0.008 and 50 Hz), a Kinematrics FBA-23 strong motion accelerometer, and a Teledyne broadband KS-54000 (passband between 0.0003 and 8 Hz). The KS-54000 is emplaced in a borehole at a depth of 100 m to insure the quietest possible recording environment. The purpose of installing the STS-2 is to provide much better coverage of high frequencies than would be possible with the KS-54000 alone. The FBA-23 is in place to record ground motion from earthquakes either too large or too close to be recorded on-scale by the KS-54000 and STS-2. All sensors are recorded on an IRIS-3 high-resolution data acquisition system.

The IRIS/IDA station RAYN has noise characteristics which place it among the quietest seismic stations in the world. Minimum detectable magnitudes are estimated for RAYN station using the observed noise levels over 1 Hz. The m_b detection threshold for the distance range of 5–10° is about $m_b = 2.7–3.0$ assuming the signal-to-noise ratio of 3 dB or better.

Results and Data Analysis

Seismic Noise Measurements

Background seismic noise is an unavoidable problem in earthquake monitoring. The amplitudes of seismic arrivals decrease with distance and seismic magnitude. Path propagation effects, such as attenuation and elastic structure lead to variability in seismic amplitudes. Noise inhibits the detection of weak seismic arrivals (phases) from distant and/or small events. Seismic noise is generated from a variety of sources. These include both man-made (e.g. roads, machinery) and natural sources (e.g. wind, ocean waves, temperature effects). Noise properties can vary between daylight and night hours and between seasons (e.g. summer and winter). Also the geologic character of the seismometer placement has great effect on the noise–hard rock sites typically have lower

Table 14.1 KACST digital seismographic stations network

Station code	Station location	Latitude	Longitude	Elevation (meters)	Sensor type
AFFS	Afif	23.9267	43.0005	109	BB
ALWS	As Safayhah	29.3103	35.0650	0	SP
ARSS	Ar Rass	25.8810	43.2365	72	BB
AYUS	Aynunah	28.1889	35.2689	0	SP
BDAS	Al Bada	28.4317	35.1014	36	BB
BIDS	Al Bida	26.8670	36.9595	0	BB
BLJS	Baljurashi	19.8812	41.5992	206	BB
DBAS	Duba	27.2114	35.9773	18	SP
DJNS	Dahran-Al-Janub	17.7073	43.5434	220	BB
FRAS	Faraa	21.0622	40.5200	0	BB
FRJS	J.-Farasan	22.5905	39.3638	0	SP
FRSS	Farasan Island	16.7392	42.1143	0	BB
HAQS	Haql	29.0548	34.9297	42	BB
HASS	Al Hasa	25.1899	49.6944	20	BB
HILS	Al Hail	27.3835	41.7917	108	BB
HKNS	J.-Hakran	22.6420	41.7158	0	SP
HWYS	Hawiyah	21.4349	40.4177	0	SP
JAZS	Jizan	17.0678	42.9177	0	SP
JMOS	J. Al-Moallq	29.1686	35.1094	0	BB
JMQS	J. Al-Moqyreh	28.8861	35.8778	0	BB
KAMS	Al Khamasin	20.3092	44.5798	75	SP
KBRS	Harrat Khaybar	25.7893	39.2623	78	BB
LBNS	J. Laban	21.0465	39.9013	0	BB
LTHS	Al Lith	20.2750	40.4107	18	BB
MOHS	Muhayl	18.5761	42.0190	52	BB
MYKS	Mirrayikh	21.5545	39.3323	0	SP
MZLS	Mezel	24.0275	45.2071	88	SP
NAJS	Najran	17.5034	44.2847	131	BB
NAMS	Namsa	19.1714	42.2084	252	BB
QURS	Al Hadithat	31.3860	37.3240	49.1	BB
RNYS	Wadi Ranyah	21.4267	42.7662	0	SP
RYDS	Riyadh	24.1900	46.6400	0	BB
TATS	Tathlith	19.5412	43.4775	110	BB
TAYS	Tayyib Ism	28.5511	34.8717	0	BB
TBKS	Tabuk	28.2248	36.5485	82	BB
UMJS	Umm Lajj	25.2340	37.3119	13	SP
WBHS	Wadi-Ibnhashbal	18.6057	42.7144	187	SP
YNBS	Yanbu	24.3397	37.9922	8	BB

noise levels than sites on weathered or sedimentary rock or unconsolidated material. Because of the variety of noise sources and the variability of noise, propagation and site characteristics at network sites, the noise properties at seismic stations are frequency dependent and can be highly variable between sites.

Noise spectra were measured at KACST stations (AFFS, HASS, HILS, QURS and TATS). Event-segmented data were previewed and first arriving P-waves were picked. Waveforms were instrument corrected to absolute ground motion using the LLNL developed Seismic Analysis Code (SAC). Noise segments were taken as the available waveform before the

Fig. 14.3 Noise spectra at station AFFS. Acceleration power spectra (in decibels relative to 1 m2/s4) are shown for the vertical, north and east components. Individual spectra are shown in *red* and the average spectra in *black*. Also shown are the average low and high noise spectra (*dotted line*) of Peterson (1993)
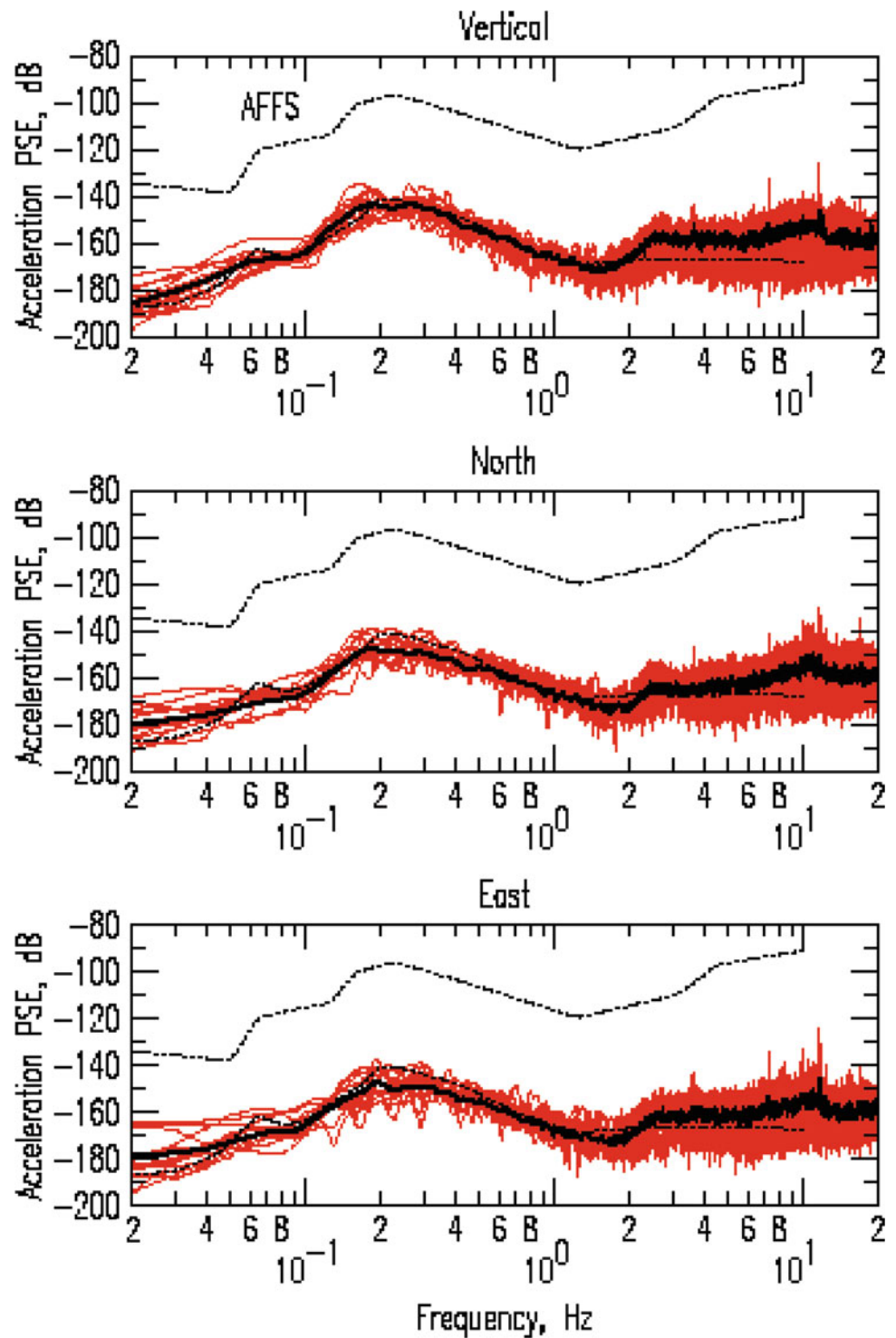
P-wave pick. Typically for SANDSN data this was 30–60 s. For noise spectral measurements we accepted only segments 30 s or longer. This limited the low-frequency resolution of our noise estimates. Power spectral densities were computed for noise windows by Fast Fourier Transform (FFT) and normalized by the window length. Noise spectra are presented in acceleration in decibels relative 1 $(m/s^2)^2/Hz^2$.

Indicatively, the noise at AFFS station is presented in Fig. 14.3 showing the vertical, north and east component noise acceleration power spectra (in decibels relative to 1 m^2/s^4). Also shown are the average low and high noise spectra as in Peterson 1993).

Results showed that stations AFFS, HILS and TATS have the lowest noise levels. Stations HASS and QURS

have the highest noise levels of the sites considered. Cultural noise appears as spikes in the power spectra at frequencies above 1 Hz. This is most notable at stations HILS (4 and 8 Hz) and QURS. These sites may be affected by nearby cultural noise sources, such as roads and human activities.

Generally the noise is relatively low amplitude between 0.1 and 1 Hz, except for station HASS. Detection of energy at frequencies around 1 Hz is most important for P-wave arrivals used in the event location. Higher frequency energy is useful for detecting local and regional events, less than 1,000 km away.

SANDSN Location Performance

The locations of the events outside the network were improved by calibrating the travel time or velocity structure between the event regions and recording stations. The arrival times of moderate-sized events ($m_b \geq 4.5$) can be accurately measured to uncertainties of 1 s or less, if noise levels allow for good signal-to-noise levels. The calibration task is made difficult by the fact that one often does not accurately know the location and origin times of events. Events with accurate locations and origin times, so called ground truth (GT) events, are difficult to obtain. GT events come in various varieties. Man-made explosions with controlled location and detonation time are the best and most difficult to obtain form of ground truth. These events can be located with uncertainties of less than 100 m and the origin times can be determined to tenths of a second. Mining and civil engineering explosions can be good sources of ground truth, however, these events are often too small to be observed beyond 100 km. Earthquakes excite more seismic energy and can be observed at larger distances, however, their locations are poorly more constrained. In some cases where an earthquake is recorded at local distances (<100 km) with good azimuthal coverage, the locations can be accurate to less than 10–20 km (Sweeney 1996). This translates to 1–2 s of travel time at regional distances.

Comparison with Catalog Locations

Earthquake locations for events in and around Saudi Arabia were then compared with those reported by networks with global station coverage (e.g. REB, USGS-PDE and ISC). The comparison first associates events from each catalog in the LLNL Seismic Research Database. Event locations must occur at nearly the same time and location to be associated with the same event. The global catalogs have the advantage of global azimuthal coverage of each event, while the SANDSN network has observations limited to stations within the Kingdom of Saudi Arabia. Most of the seismicity occurs near or outside the borders of the Kingdom, making location strongly dependent on the assumed seismic velocity model and travel time curve(s).

The KACST station locations were compared with those reported by: the Provisional Technical Secretariat (PTS) of the Comprehensive Test Ban Treaty Organization (CTBTO) Reviewed Event Bulletin (REB); International Seismological Center (ISC) and the United States Geological Survey (USGS) National Earthquake Information Center (NEIC) Preliminary Determination of Epicenters (PDE). These organizations report seismic event catalogs based on worldwide observations of body-wave arrival times. We restricted the global catalog event magnitudes to be 4.0 or greater. This reduces small events that might be poorly observed and located by the global network(s). Figure 14.4 shows the comparison of event locations from the KACST and global network bulletins for the Zagros Mountains region. The map shows that the KACST station locations were generally to the southwest of the global network locations. The mean location (epicenter) difference is over 50 km. This corresponds to travel time error of as much as 6 s. Similar analysis was preformed on a very limited set of Red Sea events. The location differences do not appear to be very large for the events studied. There are not many large events in this area.

These location differences are probably due to the velocity model errors and can be reduced by using more appropriate region dependent velocity models instead of the *iasp91* model. The *iasp91* model is a global average model for continental regions and is most accurate for predicting teleseismic travel times. At local to regional distances (0–1,500 km) travels times are strongly region dependent due to lithospheric structure (i.e. crustal thickness, crustal and uppermost mantle seismic velocities and attenuation). These variations also lead to differences in regional phase amplitudes and propagation characteristics and require detailed study beyond the scope of the current project.

Improved Velocity Models for the Arabian Peninsula

The sensitivity of travel times to one-dimensional (1D) average velocity structure is certainly non-unique and the goal was to find a range of models that fit the data reasonably well and are consistent with what is already known about the region. By using a grid search technique the problems associated with linearizing the dependence of the data on model parameters were, as avoided required by linear inversion methods. The grid search was performed using travel time data sets: (1) Pn and Pg, and (2) Pn, Pg and Sg. Two data sets were considered for two reasons. Firstly, the onset times of Sg

Fig. 14.4 Statistical
characterization of location
differences between KACST and
global network locations for the
Zagros Mountains region: (*top*)
azimuth and distance; (*left*)
epicentral difference; (*right*)
directional bias in locations
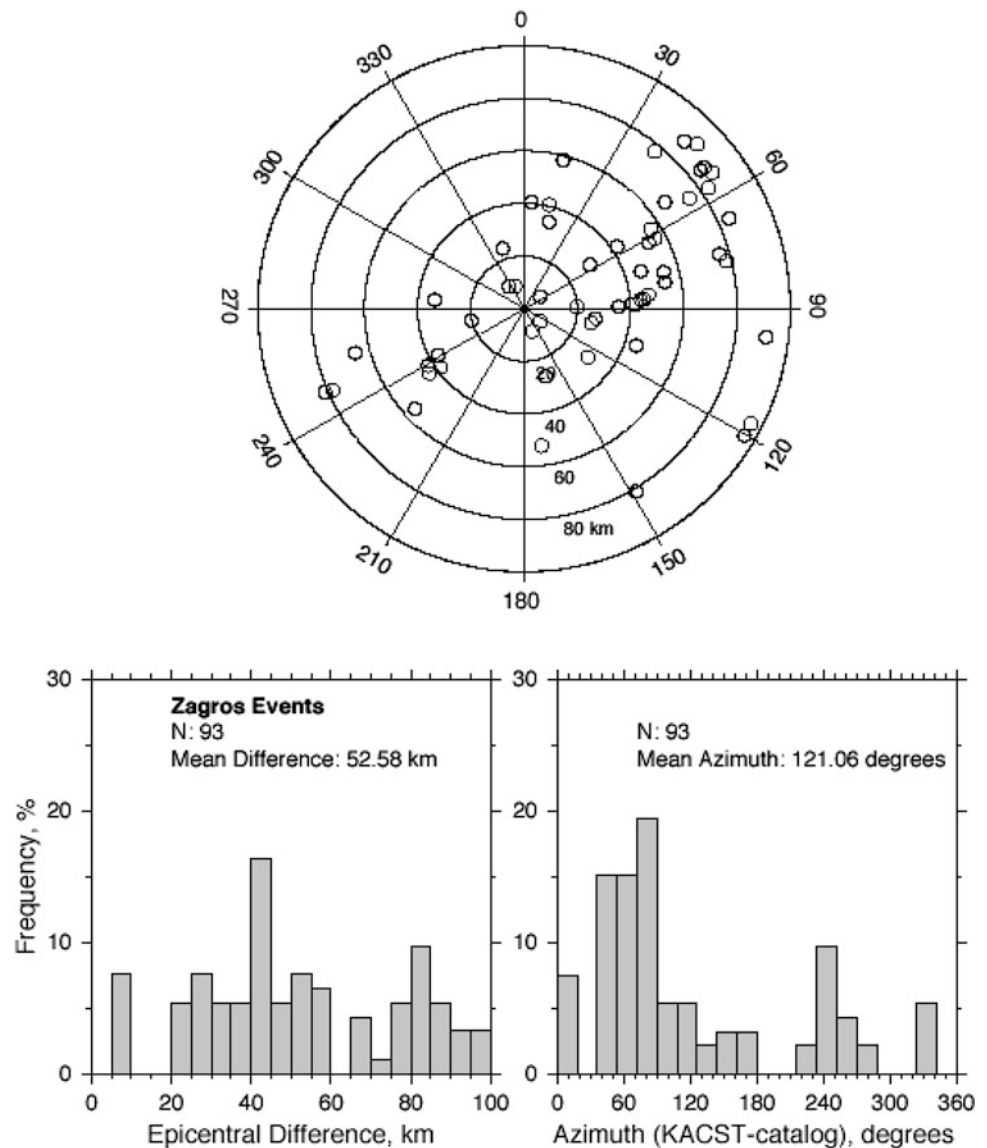
are more difficult to pick, so it may not be prudent to include
the Sg picks in the estimation of structure.

Secondly, there is direct solution for the shear wave
velocities, but rather scaling shear velocities to compres-
sional velocities with an assumed Poisson's Ratio, so the
influence of Sg travel times may bias the model. The
optimal model should reduce the scatter in the data
(i.e. minimize the rms) and result in zero-mean residuals.
The models were chosen that resulted in absolute mean
residuals less than 0.5 s and minimum rms. The threshold
on the absolute mean residual was chosen to be a conser-
vative estimate on the picking error. From the 800 models
considered, were chosen. The 20 best fitting models
according to the criteria described above. Crustal thick-
nesses range between 24 and 30 km. The upper crustal
velocities are poorly resolved by both data sets. Velocities
of the lower crust are 6.0–6.2 km/s.

Discussion and Interpretation

Travel Times Calibration

The best data for calibrating travel times to improve
earthquake location are well-coupled controlled source
explosions. These experiments use buried explosive sources
with well known location and origin time to generate seis-
mic waves that can be observed at large ranges. In
November 1999, two such explosions were conducted in the
Dead Sea (Gitterman and Shapira 2002). These explosions
were well-recorded to about 500 km distance by KACST
stations in the Gulf of Aqabah and northwestern Saudi
Arabia. Details of the explosion location, origin time and
yield are given in Table 14.2. Both shots were detonated in
the water at 70–73 m depth. A smaller shot (500 kg) was

Table 14.2 Ground truth locations (Gitterman and Shapira 2002)

Latitude	Longitude	Date	Time (GMT)	Yield (kg TNT)
31.5338	35.4400	Nov. 10, 1999	13:59:52.210	2060
31.5336	35.4413	Nov. 11, 1999	15:00:00.795	5000

Table 14.3 Automatic locations of dead sea shots by KACST network

Latitude	Longitude	Date	Time (GMT)	Mislocation (km)
31.6214	35.1506	Nov. 10, 1999	13:59:58.807	29.1
31.8143	35.0178	Nov. 11, 1999	14:59:58.572	50.7

Table 14.4 Velocity model for the Gulf of Aqabah/dead sea region

Depth (km)	Thickness (km)	V_P (km/s)	V_S (km/s)
0	2	4.50	2.60
2	5	5.50	3.18
7	10	6.10	3.52
17	11	6.20	3.60
28	∞	7.80	4.37

conducted on November 8, 1999, but we did not analyze the data because the signal-to-noise was poor on the Saudi networks.

The KACST system detected and located the events, however their locations are quite far from the known (ground truth) locations as indicated in Table 14.3.

Generally, explosions are detected and located by regional networks and range in magnitude up to m_b 3.5. Events of this type are of interest to regional network operators and nuclear monitoring researchers for several reasons. First, they pose a significant detection, association and location load to nearby stations and networks. Second, chemical explosions can have similar characteristics to underground nuclear explosions (such as the absence of low-frequency S-wave energy) and can fail event screening and discrimination tests. This can place a significant processing load on nuclear treaty monitoring systems. Finally, mining events can be useful for monitoring because they can provide valuable calibration data for event location and characterization. If one knows the location and origin time of mining explosions, then the recordings can be used to calibrate path-dependent travel times.

Velocity Models from Surface Wave Dispersion and Waveform Modeling

Earlier work with waveform data from the 1995–1997 Saudi Arabian Broadband Deployment by the University of California, San Diego (UCSD) and King Saud University resulted in models for the Arabian Platform and Arabian Shield (Rodgers et al. 1999). In that study, Love and Rayleigh wave group velocities were modeled to estimate average one-dimensional seismic velocity models of the two main geologic/tectonic provinces of Saudi Arabia. A grid search was used to quickly find a range of models that satisfactorily fit the dispersion data, then that range of models was explored to fit the three-component broadband (10–100 s) waveforms. The resulting models revealed significant differences between the lithospheric structure of the three regions as shown in Tables 14.4, 14.5, and 14.6.

Surface Wave Group Velocity Analysis

To check the validity of our model for the Arabian Platform, Rayleigh and Love wave group velocities were measured for a number of regional events from the Zagros Mountains and Turkish-Iranian Plateau. Paths from these events to KACST stations sample the Arabian Platform and also shown the predictions of the Arabian Platform velocity model (Rodgers et al. 1999). A tomographic model of surface wave group velocities was constructed for the Arabian Peninsula and Africa Rift regions by Benoit et al. 2002. Figure 14.5 shows the resulting tomographic image of 20 s Rayleigh wave group velocities. The image shows slower than average velocities for the Arabian Platform and Rub Al-Khali, probably due to low velocity sediment cover. The Red Sea is faster than average due to thinner crust. The 20 s group velocities gradually increase from the Eastern

Table 14.5 Velocity model for the Arabian shield region

Depth (km)	Thickness (km)	V_P (km/s)	V_S (km/s)
0	1	4.0	2.31
1	15	6.20	3.58
16	20	6.80	3.93
36	∞	7.90	4.30

Table 14.6 Velocity model for the Arabian platform region

Depth (km)	Thickness (km)	V_P (km/s)	V_S (km/s)
0	4	4.00	2.31
4	16	6.20	3.64
20	20	6.4	3.70
40	∞	8.10	4.55

V_P and V_S, are the P- and S-wave velocities, respectively

Province to the Hejaz and Red Sea. The inclusion of additional surface wave dispersion data could help resolve three-dimensional structure of Saudi Arabia.

Evaluation of SANDSN Timing with P-Wave Arrival Times

In order to check the timing at the SANDSN stations and to measure relative P-wave arrival times we used an accurate cross-correlation method (Al-Damegh et al. 2005). This method finds the optimal relative timing of vertical component P-waves at a set of stations. The travel time residuals were then computed relative to a layered earth model, such as *iasp91* (Kennett and Engdahl 1991). This method was used by Benoit et al. (2002) to image P-wave velocity anomalies beneath the Arabian Shield. Residual uncertainties are typically 0.05–0.1 s. The method was to check the relative timing of the KACST stations to identify possible timing errors at the stations. Modern seismic recording systems use GPS timing at the site and are less likely to have problems compared with older systems. The residuals were quite small ranging about 1.5 s. This range was consistent with that found by Benoit et al. (2002) and is likely related to upper mantle P-wave velocity structure and not due to timing problems at the stations.

Evaluation of Velocity Models with Sandsn Travel Times

The seismic velocity models described above are emblematic of the variability in thermal and compositional structure related to complex tectonic processes at work in the Arabian Peninsula. In order to check the
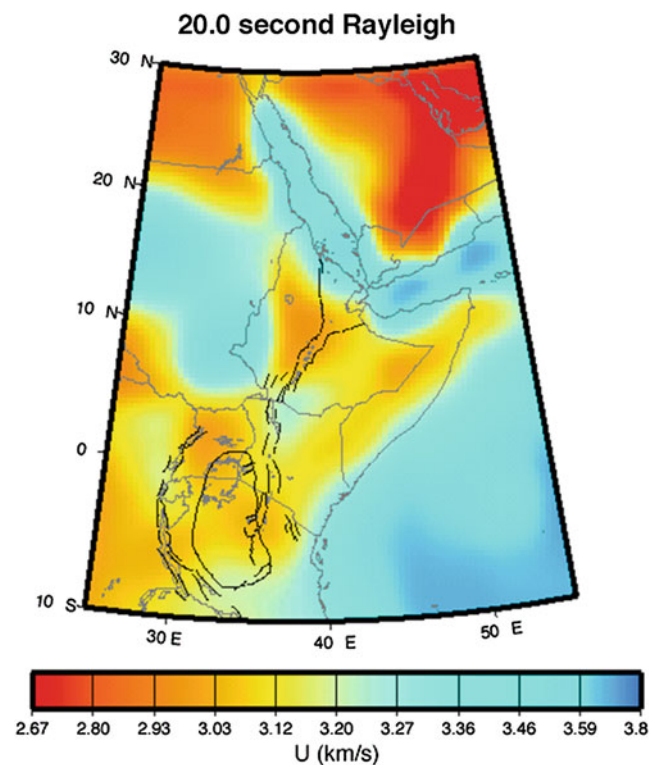

Fig. 14.5 Rayleigh wave group velocities at 20 s for the Arabian Peninsula, African Rift and surrounding regions

validity of travel time predictions from our proposed seismic velocity models, a comparison was made for the observed travel times for well-located earthquakes and chose to use waveforms from the 1995–1997 UCSD-KSU Saudi Arabian Broadband Deployment. This was decided for two reasons. Firstly, due to the limited KACST waveform data to work with. Secondly, we used the earthquake locations from the International Seismological

Fig. 14.6 Focal mechanism and scaled error versus depth for the individual three-component station data (**a–c**, HASS, KBD and ABKT, respectively) and the joint fitting of all three stations (**d**)
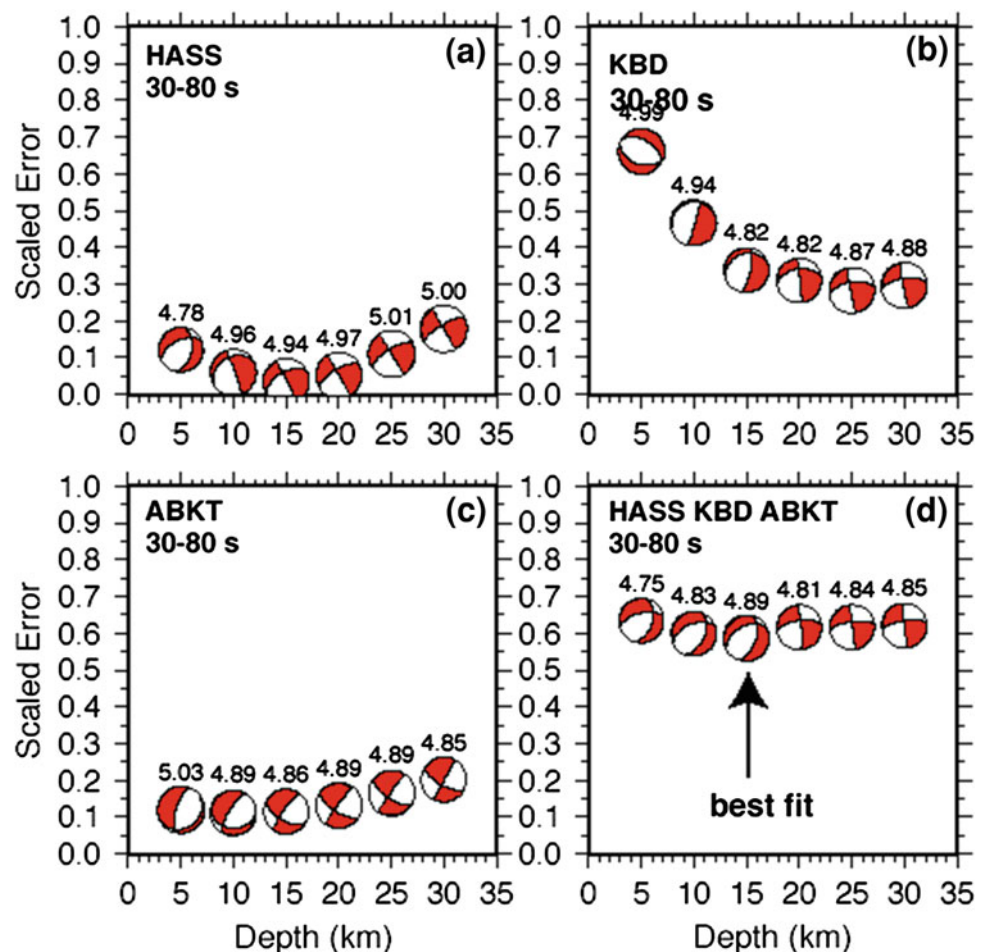
Center (ISC). These locations rely on arrival time reports from all over the world and their publication availability is delayed by more than 2 years. There was little or no overlap between our well-located earthquake catalog and KACST data holdings. The available catalog had events in the Zagros Mountains. This provided paths sampling the Arabian Platform. Agreement between the observations and the Arabian Platform model predictions is quite good. The paths sample the faster crust of the Arabian Shield and this may be the reason that the arrivals are on average early compared with the model predictions.

Focal Mechanisms of Regional Events

A moderate (M ∼ 5) earthquake struck the northeastern United Arab Emirates (UAE) on March 11, 2002. The event was large enough to be detected and located by global networks at teleseismic distances. The region is generally believed to be aseismic, however no regional seismic network exists in the UAE to determine earthquake occurrence. This event served as a test case to illustrate the KACST station location performance and demonstrated what can be

done with broadband waveform data. Local information provided by the United Arab Emirates University (UAEU) Department of Geology, locates this event in or near the town of Masafi, in the Oman Mountains.

Broadband complete regional waveforms were used to estimate a focal mechanism and depth of the event. Figure 14.6 shows the misfit (scaled error) and focal mechanism versus depth for the individual stations (HASS, KBD and ABKT) and for the combined three-station fit. The focal mechanism is consistent with the broad-scale tectonics of the Arabian-Eurasian collision. To the west to the Musandam Peninsula, Arabia is under thrusting the southern Eurasian margin along the Zagros Thrust. To the east of the Musandam Peninsula, convergence is much slower given the seismicity along the Makran coast. Strike-slip motion probably occurs along reactivated thrust planes associated with obduction of the Semail Ophilite (Oman Mountains).

Conclusions

- The sites are quiet and noise surveys at a few stations indicated that seismic noise levels at KACST stations are

quite low for frequencies between 0.1 and 1.0 Hz, however cultural noise appears to affect some stations at frequencies above 1.0 Hz. Broadband waveform data is generally comparable with data from the Global Seismic Network operated by the Incorporated Research Institutions for Seismology (IRIS-GSN).

- No Evidence was found of timing problems with the data. The sample rate (currently set at 100 samples/second) can be lowered to 50 samples/second without any loss of information. The current high sample rate has several unwanted consequences. Firstly, the high sample rates taxes network communications and computational facilities. Secondly the high sample rate requires additional memory requirements when the data are archived. Reducing the sample rate to 50 would immediately reduce the load on tape and disk memory by 50 %.

- The ANTELOPE system appears to be operating as expected, routinely detecting and locating events. However, the location errors described above are the result of using an inappropriate velocity model. The system uses the *iasp91* model (Kennett and Engdahl 1991). While this model is probably adequate for locating distant (teleseismic) events in continental regions, it leads to large location errors, as much as 50–100 km, for regional events.

- Variability of lithospheric structure is revealed by the need for different models for the regions of the northwest of Saudi Arabia (the Gulf of Aqabah/Dead Sea), the Arabian Shield and the Arabian Platform. Travel time analysis and surface wave group velocities confirm the variability in structure and the need for path-dependent models.

- We measured surface wave group velocities for a number of earthquakes with paths sampling the Arabian Platform. Inclusion of these measurements in a tomography study shows a rich pattern of structure.

References

Al-Amri AM (1998) The crustal structure of the western Arabian Platform from the spectral analysis of long-period P-wave amplitude ratios. Tectonophysics 290:271–283

Al-Amri A (1999) The crustal and upper-mantle structure of the interior Arabian platform. Geophys J Int 136:421–430

Al-Amri A, Mellors R, Vernon F (1999) Broadband seismic noise characteristics of the Arabian Shield. Arab J Sci Eng 24(2A):99–113

Al-Amri MS, Al-Amri AM (1999) Configuration of the seismographic networks in Saudi Arabia. Seism Res Lett 70:322–331

Al-Damegh K, Sandvol E, Barazangi M (2005) Crustal structure of the Arabian plate: new constraints from the analysis of teleseismic receiver functions. Earth Planet Sci Lett 231:177–196

Benoit M, Nyblade A, Van Decar J, Gurrola H (2002) Upper mantle P wave velocity structure and transition zone thickness beneath the Arabian Shield. Geophys Res Lett 30

Debayle E, Lévêque J, Cara M (2001) Seismic evidence for a deeply rooted low-velocity anomaly in the upper mantle beneath the northeastern Afro/Arabian continent. Earth Plan Sci Lett 193:423–436

Gettings M, Blank H, Mooney W, Healey J (1986) Crustal structure of southwestern Saudi Arabia. J Geophys Res 91:6491–6512

Gitterman Y, Shapira A (2002) Dead Sea seismic calibration experiment contributes to CTBT monitoring. Seismo Res Lett 72:159–170

Jackson J, Fitch T (1981) Basement faulting and the focal depths of the larger earthquakes in the Zagros mountains (Iran). Geophys J R Astron Soc 64:561–586

Kennett B, Engdahl E (1991) Travel times for global earthquake location and phase identification. Geophys J Int 105:429–465

Mellors R, Vernon F, Camp V, Al-Amri A, Gharib A (1999) Regional waveform propagation in the Saudi Arabian Peninsula. J Geophys Res 104(B9):20221–20235

Mokhtar T, Al-Saeed M (1994) Shear wave velocity structures of the Arabian Peninsula. Tectonophysics 230:105–125

Mooney W, Gettings M, Blank H, Healy J (1985) Saudi Arabian seismic refraction profile: a traveltime interpretation of crustal and upper mantle structure. Tectonophysics 111:173–246

Peterson J (1993) Observations and modeling of seismic background noise. U.S. Geological Survey Open-File Report 93–322, Albuquerque, NM, p 94

Randall G (1994) Efficient calculation of complete differential seismograms for laterally homogeneous earth models. Geophys J.Int 118:245–254

Ritsema J, Van Heijst F, Woodhouse J (1999) Complex shear wave velocity structure beneath Africa and Iceland. Science 286:1925–1928

Rodgers A, Walter W, Mellors R, Al-Amri A, Zhang Y (1999) Lithospheric structure of the Arabian shield and platform from complete regional waveform modeling and surface wave group velocities. Geophys J Int 138:871–878

Sandvol E, Seber D, Barazangi M, Vernon F, Mellors R, Al-Amri A (1998) Lithospheric velocity discontinuities beneath the Arabian shield. Geophys Res Lett 25:2873–2876

Seber D, Mitchell B (1992) Attenuation of surface waves across the Arabian peninsula. Tectonophysics 204:137–150

Sweeney J (1996) Accuracy of teleseismic event locations in the Middle East and North Africa, Lawrence livermore national laboratory informal document, UCRL-ID-125868

Vernon F, Berger J (1997) Broadband seismic characterization of the Arabian Shield. Final Scientific Technical Report, Department of Energy Contract No. F 19628-95-K-0015, p 36

Walter W (1993) Source parameters of the June 29, l992, little skull mountain earthquake from complete regional waveforms at a single station. Geophys Res Lett 20:403–406